Restoration of thermal images distorted by the atmosphere, based on measured and theoretical atmospheric modulation transfer function

Dan Sadot, MEMBER SPIE
A. Dvir
I. Bergel
Norman S. Kopeika, MEMBER SPIE
Ben-Gurion University of the Negev
Department of Electrical and Computer Engineering
Beer-Sheva, Israel
E-mail: kopeika@bguee.bgu.ac.il

Abstract. Restoration of thermal images distorted by the atmosphere is presented. The method is based on atmospheric MTF analysis, both theoretical and experimental. Thermal IR atmospheric MTF measurements performed simultaneously in both atmospheric IR windows (3- to 5- and 8- to 12-μm wavelengths) are also presented. The MTFs were evaluated via point spread function measurements, under various meteorological conditions and different SNRs. Results are analyzed and shown to be in very good agreement with theoretical predictions.

Subject terms: infrared technology; image restoration; modulation transfer function; atmospheric measurements; aerosols; atmospheric optics; thermal imaging.

Optical Engineering 33(1), 44–53 (January 1994).

1 Introduction

Thermal imaging systems have progressed significantly in recent years. New focal plane array technology similar to CCD arrays in the visible range permits high-resolution imaging; however, when dealing with long-distance imaging through the atmosphere, system performance is often limited due to the atmospheric distortions. Usually, the atmospheric effect in the thermal range is referred to in target acquisition models[1] as a constant attenuation via the Beer-Lambert law. No treatment is considered for the spatial frequency dependence of the atmospheric effect, i.e., the atmospheric MTF; however, recent analysis,[2,3] applying some practical limitations to the "classical" theory, predicts significant atmospheric MTF variation with spatial frequency also in the thermal range, which is in very good agreement with results presented in this paper. These results suggest that target acquisition probabilities are effected much more adversely by the atmosphere for small targets than for large targets. These results disagree with target-acquisition modeling, which assumes no atmospheric spatial frequency dependence. Knowledge of atmospheric MTF is essential to good system design. It is also very useful in image restoration for any type of target or object.

A general configuration of the problem of imaging through the atmosphere is illustrated in Fig. 1. The source of radiation is in the object plane, which is a point source that produces a spatial delta function in this example. The atmosphere is a random medium that contains both turbulence and scattering and absorbing particles. At the other end of the atmospheric path is the imaging system, which includes both the optics and electronics. The main effect of the turbulent medium is to produce a wavefront tilt as illustrated in Fig. 1, which causes image shift at the image plane. These tilts are random and their temporal power spectra are usually limited to several tens and up to a few hundred hertz in ordinary atmospheric conditions. The image distortions caused by the wavefront tilt (typically of the order of tens or maybe hundreds of microradians) can be compensated for either by adaptive optics techniques or by means of software if the exposure time is short enough—less than the characteristic fluctuation time (usually a few milliseconds). A blur effect related to turbulence also occurs (not illustrated in Fig. 1), which usually affects very high spatial frequencies. This blur effect can be characterized by the well-known turbulence short exposure MTF.[4]

In addition to turbulence, scattering and absorption effects exist produced by molecules and aerosols. Scattering gives rise to a very wide diffusion of the point object radiation, as shown in Fig. 1. This causes a wide variance in the angle of arrival according to the particulate scattering phase function and, thus, also produces blur at the image plane. Unlike the short exposure turbulence case, the blur due to aerosols is very wide, usually of the order of radians, which is orders of magnitudes wider than the imaging system field of view; moreover, there are some practical limitations that should be applied to the scattered light recorded in the image. The angular spread of the incident scattered light is approximately of the order of λ/a, where a is the dominant particulate radius and λ is the radiation wavelength. In the atmosphere in the thermal IR range, this angular spread of scattered light is of the order of several radians, and will usually be truncated by the imaging system field-of-view limitation, which may be typically of the order of milliradians. Therefore, not all the scattered light will appear at the image plane. Furthermore, even if it does reach the detector, the entire amount of scattered radiation will not necessarily be detected by the sensor. The reason for this is that every detector has a limited dynamic range, and scattered radiation of very low intensity compared to the unscattered light will not be detected at all. The weak intensity scattered light is at larger scatter angles. Thus, dynamic range limitations of the imaging system also limit scatter angles recorded in the image, often even more so than the field of view. In addition, the dynamic range might be limited by the SNR of the scene itself. If the scattered light

Paper IRT-21 received June 6, 1993; revised manuscript received July 23, 1993; accepted for publication July 24, 1993.

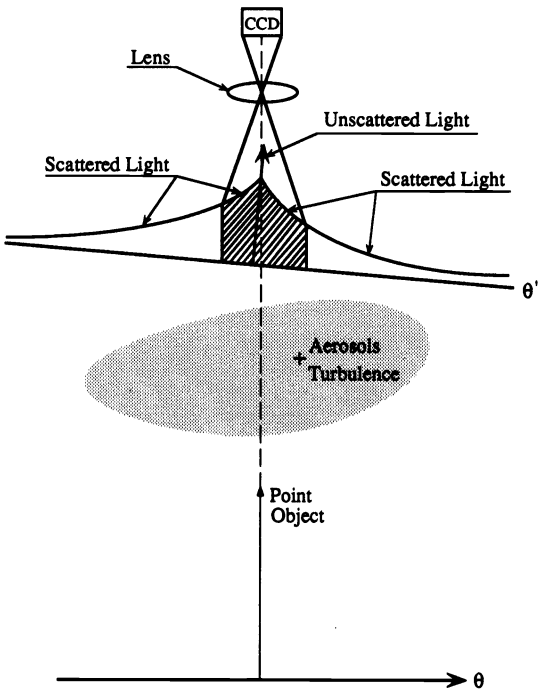

Fig. 1 Relations between atmospheric distortions and imaging system limitations.

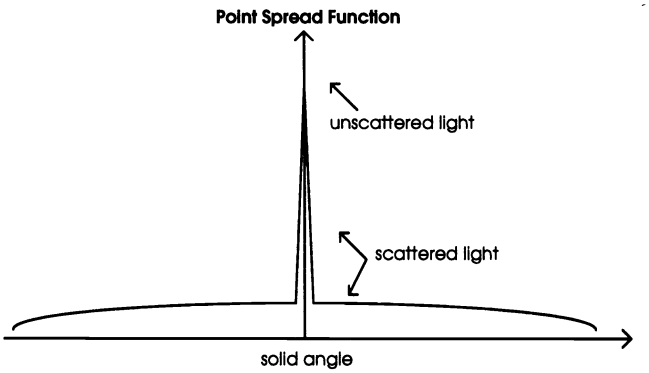

Fig. 2 Typical particulate scattering pattern.

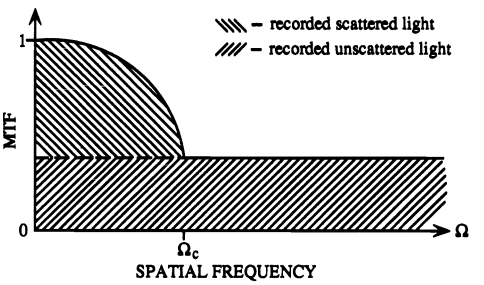

Fig. 3 Typical aerosol MTF.

is at irradiance levels lower than that of the background irradiance, its contribution to the blur effect will be minor and usually negligible.

In addition, practical limitations must be applied also to the unscattered component of the radiation. The finite angular spatial frequency bandwidth truncates the high angular spatial frequency radiation, because unscattered light from a point object is equivalent to a constant of infinite spectrum in the angular spatial frequency plane. Limited spatial frequency bandwidth of the sensor limits the amount of unblurred or unscattered light actually recorded in the image.

All the practical instrumentation limitations should be applied to the classical theory dealing with aerosol MTF, as summarized in Ref. 2.

The absorption effect should also be taken into account. In the thermal IR range, the absorption effect is very dominant, unlike in the visible range. The light reaching the imaging system of Fig. 1 contains both unscattered and scattered components. In the far infrared, for moderate atmospheric conditions, most of the scattered light, to a good approximation, is due to single scattering events. This is in view of a long wavelength and typically smaller scatterers, which give rise to smaller scattering coefficients than in the visible range. This assumption leads to the conclusion that most of the scattered light does not experience absorption, because only a single interaction occurred between each photon and particulate—either absorption or scattering; therefore, *light that was scattered was not absorbed.* Only the light that was unscattered was subject to absorption. Consider Figs. 2 and 3, which represent a typical particulate scattering pattern and the corresponding MTF. The unscattered light is a delta function (Fig. 2) with respect to the angular spatial domain, because it has no angular spread. Therefore, in the spatial frequency domain (Fig. 3), the unscattered light is constant for all spatial frequencies up to, in principle, infinite spatial frequency. The scattered light of Fig. 2 has a wide angular spread and, in the spatial frequency domain (Fig. 3), is a narrow function with cutoff angular frequency Ω_c. A correction must be made to the "classical" aerosol MTF, which treats absorption as a "simple" multiplicative factor to the aerosol MTF, which usually is introduced by replacing the scattering coefficient σ_s by the extinction coefficient σ_t; see, for example, Ishimaru,[5] Lutomirski,[6] and Zardecki, Gerstl, and Embury.[7] In this classical approach, the absorption effect is introduced as a constant attenuation to the aerosol MTF for all spatial frequencies; however, as explained above, the absorption effect must be applied only to the relative part of the unscattered light and not to the total incident radiation, which includes also scattered light. Figure 3 demonstrates this approach. This analysis can be interpreted in the spatial domain by the following: Consider the radiation at the image plane of Fig. 1. All the blur, which is related to the scattered light, was not attenuated by particulate absorption, which gives rise to a blurred image. On the other hand, the unscattered radiation that would give rise to an unblurred image for the infinite spatial frequency bandwidth was subject to absorption attenuation. Thus, the part of the Beer-Lambert law that relates to absorption $[\exp(-Az)]$ should be applied to it. This causes attenuation at the image plane only to the central part of the imaged point, which is related to the unscattered light, but not to the blur around it, which is related to the scattered component recorded in the image. Because the unblurred image component is attenuated by absorption and the blurred image is not, the effect of scattering is relatively enhanced by absorption, which is important in the IR. This analysis is explained extensively in Ref. 8 and ends with the final asymptotic form of aerosol MTF:

$$M_a(\Omega) = \exp\left[-S_a z \left(\frac{\Omega}{\Omega_c}\right)^2 \right] \times \exp\left[\left(\exp\left\{ -S_a z \left[1 - \left(\frac{\Omega}{\Omega_c}\right)^2 \right] \right\} - \exp(-S_a z) \right) (-A_a z) \right] , \quad \Omega < \Omega_c ,$$

$$= \exp(-S_a z) \cdot \exp\{[1 - \exp(-S_a z)](-A_a z)\} , \Omega > \Omega_c , \tag{1}$$

where Ω is the angular spatial frequency; S_a and A_a are the atmospheric scattering and absorption coefficients, respectively; z is the path length; and Ω_c is the cutoff frequency of the asymptotic aerosol MTF.[6,7] This result is illustrated in Fig. 4, which compares both the classical approach and the aerosol MTF, including the absorption angular spatial frequency dependence.

Preliminary results of measured atmospheric MTFs in the thermal range are shown elsewhere,[3] and are in good agreement with theoretical predictions. We present the extended investigation here. Results are compared at different SNRs and measured with different techniques. Also, results for different meteorological conditions are presented. Finally, based on the atmospheric MTF, restorations of images recorded along horizontal atmospheric paths are presented, indicating significant improvement in image resolution. This demonstrates the wide variety of applications that are achievable on the basis of atmospheric MTF analysis in the IR.

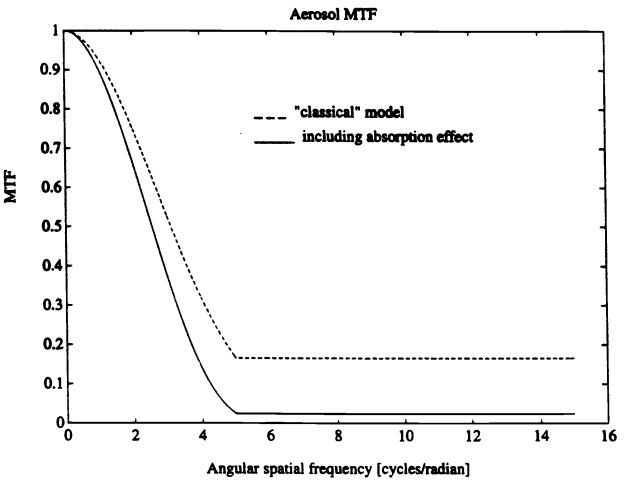

Fig. 4 Angular spatial frequency dependence of aerosol absorption on aerosol MTF.

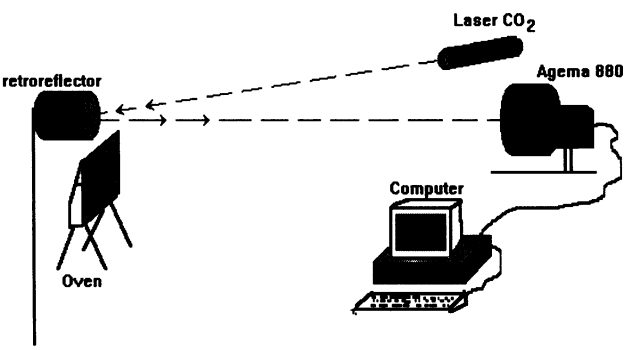

Fig. 5 Experimental setup.

2 Experiment

Two different methods were used to measure the thermal IR atmospheric MTF. Figure 5 shows the first experimental setup. This setup includes a 10-W CO_2 laser beam at 10.6-μm wavelength with a 3-mrad beam divergence. The beam was transmitted horizontally, 2-km northward, through an open laboratory window at an altitude of approximately 15 m. The beam was reflected by a hollow 12.5-cm radius corner cube retroreflector back toward a receiver, located adjacent to the transmitter. The receiver is part of an Agema thermovision model 880 IR imaging system, equipped with a 2.5-deg field-of-view telescope, and includes detectors in both atmospheric IR windows (3- to 5- and 8- to 12-μm wavelengths). Both receivers were located on stable marble optical tables located inside the laboratory, thus minimizing significantly any possible mechanical vibrations. The laser spot returning from the retroreflector was used as a coherent point source to measure the atmospheric point spread function (PSF) with the long-wave camera. This was measured by the Agema system as a point source at an equivalent temperature of 180°C. We calculated the MTF using Fourier transformation. This experiment involved a double passage through the atmosphere, which might cause the self-correction effect to be questioned. However, this effect was shown to be negligible, both experimentally[9] and theoretically,[10] mainly because the wave was diffracted at that distance.

Although we used coherent illumination as the point source in this experiment, the mutual coherence function of the radiation was strongly decayed when it reached the aperture of the imaging system because of a propagation path length of 4 km, caused by atmospheric scattering and turbulence. Using the relation between the mutual coherence function and the MTF, which are of the same shape up to an appropriate scaling,[4] we found the wave coherence diameter reaching the optics aperture to be of the order of 1 cm, while the Agema imaging system aperture diameter was 28 cm. Thus, the received laser beam is almost entirely incoherent, according to the ratio of the coherence area to the aperture area. The received incoherent laser beam radiant power is much larger than the received coherent radiant power. In this case, from any practical point of view, it can be assumed that the imaging system behaves essentially as predicted by theory for incoherent radiation, with linearity in intensity rather than field amplitude.

This type of experiment was repeated for different values of laser intensities to investigate both effects of dynamic range and SNR limitations. Results of this investigation are presented and are in very good agreement with theoretical predictions:[2]

The second experimental setup contained the same receiver, but instead of using a laser beam, we imaged a heated incoherent point source. This point source was a 50- × 50-cm-square platform that was thermally heated up to approximately 50°C. This was way above the ambient temperature,

which was not higher than 20°C. The element was located near the retroreflector; therefore, the optical path lengths of both experimental setups were identical. However, no double passage was involved in the second case. The geometrical size of the heated element was chosen such that, in the absence of atmospheric distortions, its geometrical dimensions at the image plane were less than those of a single pixel. Each pixel in the image plane corresponded to 62 × 62 cm in the object plane. The heated element thus served as a point source. MTF was evaluated with the same technique as in the first method. The second type of experiment was repeated in both IR spectral windows.

All effects of the imaging system were removed from the measured MTFs. This was accomplished by measuring the system's MTF once and, assuming no correlation existed between the system and atmospheric MTFs, the system's MTF was divided from each measurement to obtain the atmospheric MTF.

The system MTF was evaluated by measuring the image of a point source (a soldering iron) at a close distance (30 m), with essentially no atmospheric distortions. This yielded a PSF of 1 pixel, which means that the system's MTF is limited by digitization electronics to the Nyquist frequency of 1600 cycles rad^{-1}. This was confirmed experimentally via MRT measurements. In that case, the MTF is the Fourier transform of a window function corresponding to a single pixel, namely, a 2-D sinc function, which is presented in Fig. 6.

The detected intensity experimental error was negligible with a temperature resolution of 0.07°C, which leads to negligible vertical uncertainty in PSF measurements. Typical PSF images over the 2-km path were of the order of 7 to 8 pixels wide as a result of atmospheric blur. Spatial resolution error was limited to the resolution of a single pixel (0.31 mrad) divided by $\sqrt{10}$, because each experiment included an average of over 10 separate measurements, leading to a horizontal PSF uncertainty of about 4%.

During the experiments, we took measurements of standard meteorological data such as ambient temperature, relative humidity, solar flux, wind speed, and particle size distribution. The latter were measured over 0.16- to 10-μm particulate radius by means of Particle Measurement System (PMS) Inc. instrumentation.

Simultaneously, we recorded natural and urban ground scenes along the same path length (by the same thermal imaging system), which contained blur caused by atmospheric distortions. Using the measured atmospheric MTFs, we applied the image restoration techniques to the distorted images, which improved significantly the image quality. These measured atmospheric MTFs are very similar to theoretical predictions described elsewhere.[2,3]

3 Results

Typical results of atmospheric MTFs measured by the retroreflected CO_2 laser beam at various intensities are presented in Fig. 7. Note a dominant, spatial-frequency-dependent atmospheric MTF, which is in contradiction to the conventional approach that refers to IR atmospheric effects as attenuation only. This atmospheric MTF, according to shape, is attributed mainly to aerosol MTF. Turbulence is much less dominant in this experiment due to the low spatial frequencies involved, which are limited by the Agema imaging system up to 1600 cycles/rad. Using a prediction model[9] of C_n^2 based

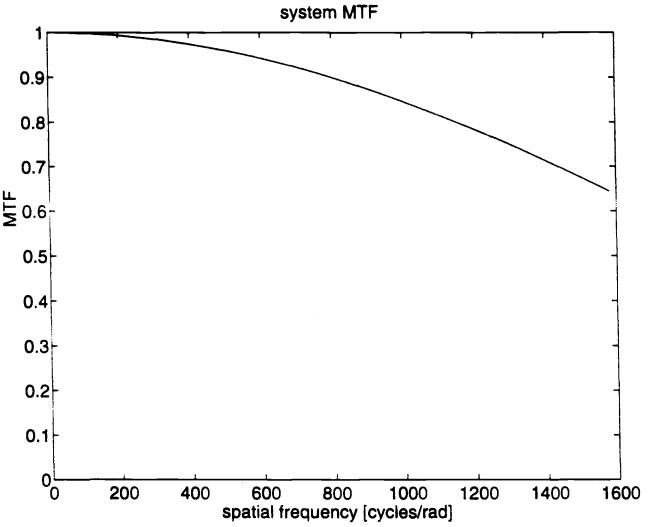

Fig. 6 System MTF.

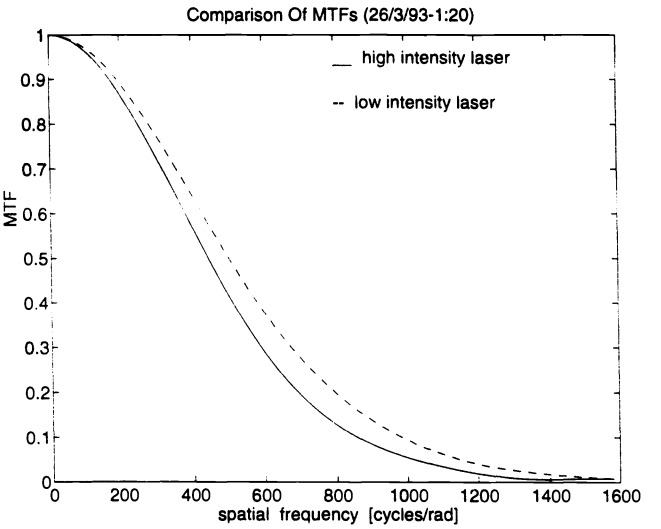

Fig. 7 Measured atmospheric MTFs for different laser beam intensities.

on basic meteorological parameters, found to be successful also in the U.S. Army Night Vision Laboratory experiments, we predicted most of the severe values of C_n^2 for the elevations considered here (~15 m) to be of the order of 5×10^{-14} $m^{-2/3}$. For the highest angular spatial frequency value (1600 cycles/rad), the worst-case turbulence MTF was over 0.95. The turbulence MTF curve is presented in Fig. 8, which indicates that it can be negligible in these experiments.

A comparison between the MTFs measured by means of the two experimental methods is presented in Fig. 9. Though measured simultaneously, the MTFs related to the heated element are generally higher than those measured by the laser beam. This result was expected theoretically[2] and is discussed in the following section.

A typical behavior of the atmospheric MTF during the day is presented in Fig. 10. Note that, in general, at night the MTF has higher values and cutoff frequencies Ω_c than during the day. This can be related to changes in the scattering

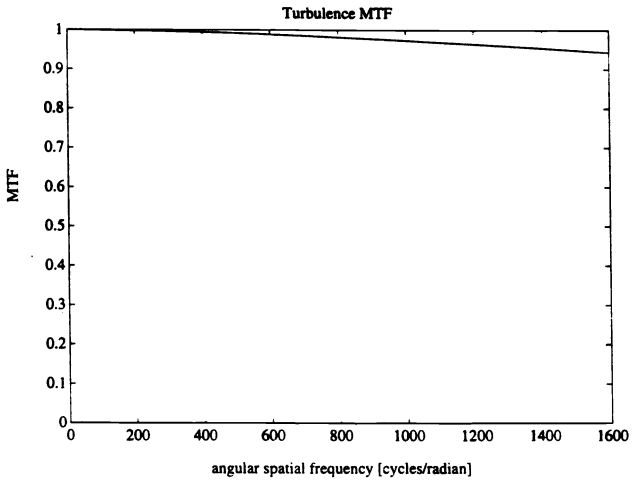

Fig. 8 Turbulence MTF.

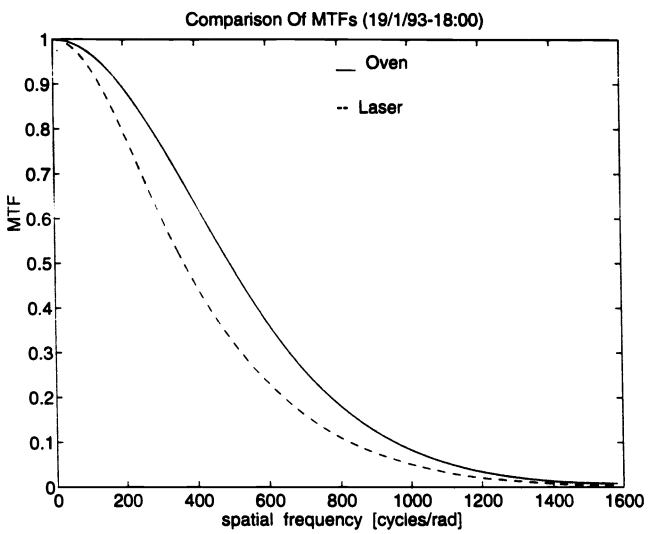

Fig. 9 Comparison between the atmospheric MTF measurements derived from the CO_2 laser beam and the heated element point source.

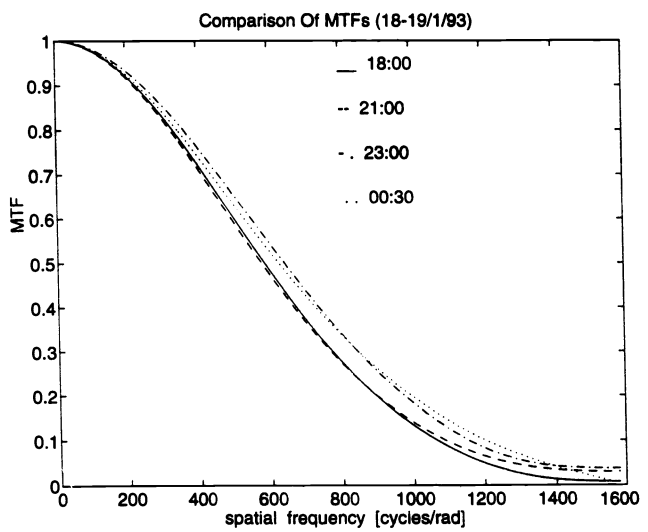

Fig. 10 Changes in atmospheric MTF during the day.

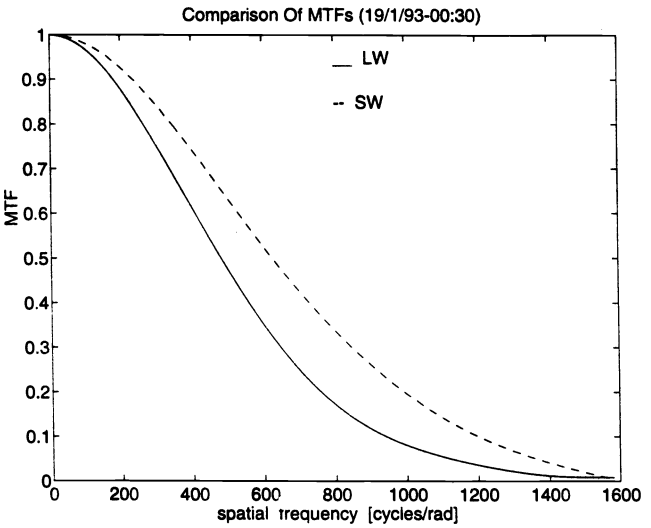

Fig. 11 Comparison between long-wave and shortwave atmospheric MTFs.

medium's phase function and is also explained in the following section.

A comparison between atmospheric MTFs in the two IR windows is presented in Fig. 11. These data were calculated via the thermal element PSF measurements. Though it seems that the shortwave atmospheric MTF is better, much lower SNRs were involved and, in general, image quality was poorer in the 3- to 5-μm range; however, better resolution should be achieved in the shortwave by means of the new focal plane array (FPA) cameras.

Figure 12 presents the entire set of MTF measurements including both IR windows. The variance in measured atmospheric MTF emphasizes that the measured MTF is significantly derived from atmospheric distortions, caused by the variety of meteorological conditions, and cannot be explained only by the system's limitations. This MTF variance is used further in some filtering techniques for image restoration.

4 Discussion

The laser beam experiment was repeated at different intensities to examine the effects of system dynamic range and SNR on the atmospheric MTF. In view of the major contribution to the atmospheric MTF by aerosol MTF, the practical aerosol MTF theory[2] was examined. In the case of low laser intensity and assuming the same background thermal noise, we expect the scattered light to be truncated at smaller angles relative to the case of high laser intensity. The lowest specific intensity to be detected by the sensor is limited either by the detector's dynamic range or by the background noise. Any scattered light arriving at intensities lower than that threshold will not be recorded in the image and, thus, will not contribute any image blur. Therefore, in the case of lower beam intensities and poorer SNRs, recorded scattered light will be of smaller scattering angles. Two effects follow in the spatial frequency domain: (1) smaller recorded scattering angles, which can be interpreted as narrower window functions in the spatial domain, are equivalent to wider convolving sinc functions in the spatial frequency domain, thus resulting in higher aerosol MTF cutoff frequencies (Ω_c in Fig. 3). (2) The more the relative amount of scattered light is trun-

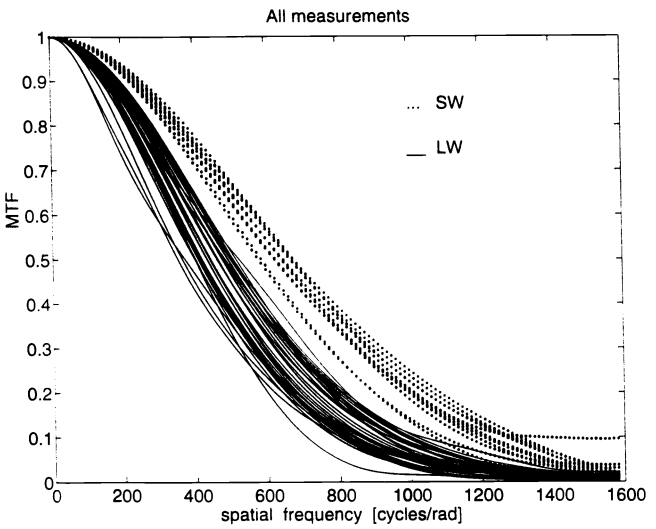

Fig. 12 Complete set of measured atmospheric MTFs.

cated, the lower the dc value or zero frequency value in the MTF domain, which is mainly due to the scattered light (as explained in Figs. 2 and 3). After normalization[2] of the MTF by its dc value, which is lower, the MTF curve will be higher, including its asymptotic value at high angular spatial frequencies.

This analysis indeed explains the results shown in Fig. 7 where, for lower laser intensities, the MTF curve was wider and higher, even though they were measured almost simultaneously. This supports one conclusion of Ref. 2, which is that limiting dynamic range yields improved spatial resolution. The comparison of results of the laser beam and thermal element in Fig. 9 shows that this effect is even more dominant because the intensity differences were greater; however, note that a wavelength difference is also involved in this comparison (10.6-μm wavelength of the laser beam and 8- to 12-μm wavelength band in the thermal element case), which might also have affected the results of Fig. 9, but not those of Fig. 7, which were found to be typical.

Another phenomena related to the aerosol MTF is the change in the MTF curves according to time of day. Generally, the particle size distribution changes between day and night usually give rise to larger particles during the night, when relative humidity increases and temperature decreases. This causes a shift in the particle size distribution toward larger particles, which results in more forward-peaked scattering phase functions during the night, which results in narrower specific intensity functions for nighttime. Applying these phenomena to the practical aerosol MTF theory[2] causes significant changes in the resulting aerosol MTF. The changes depend also on the most severe limitation between either the system's field of view or the system's dynamic range or SNR of the scene itself, as explained in the introduction. A comparison between the scattering phase functions during the day and night, for the times of MTF measurement in Fig. 10, is presented in Fig. 13(a). In this example, the phase function at 18:00 was narrower than at 00:30, which is due to the larger particles that were measured during the early evening, as presented in Fig. 13(b). This phenomenon was unusual, as mentioned previously. Figure 14 presents an illustration

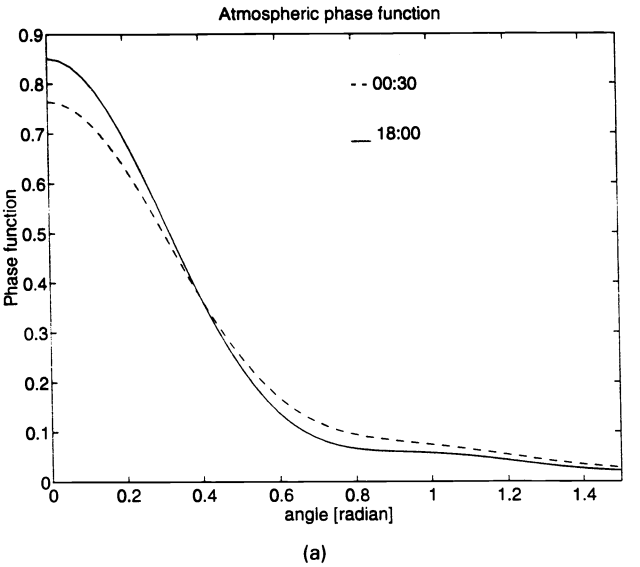

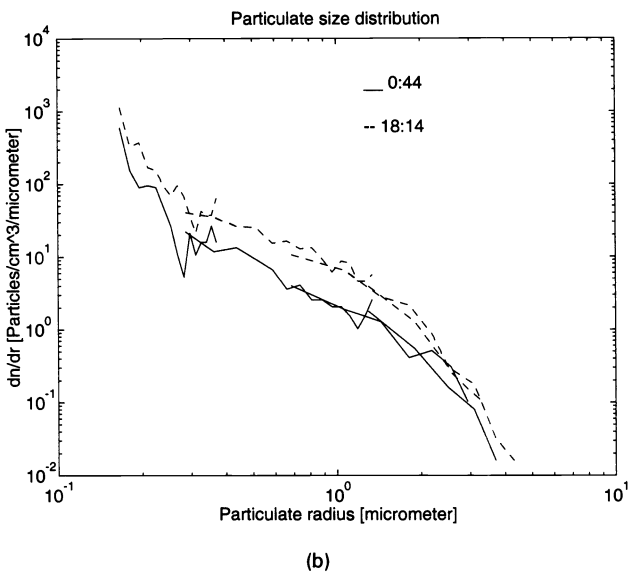

Fig. 13 (a) Comparison between phase functions during day and (b) corresponding particle size distribution, measured by the PMS instrumentation.

of this analysis applied to the specific intensity functions. The horizontal lines of Fig. 14 represent different thresholds imposed by the most severe limitations between the three parameters mentioned before, which means that intensities lower than the given threshold will not be recorded in the image. For the higher threshold, this limitation causes wider recorded scattering angles during the night (usually related to narrower scattering phase function and, thus, narrower specific intensity), resulting in a narrower MTF curve during the night; however, in the lower threshold case, the exact opposite effect occurs, namely, narrower detected scattering angles during the night, ending up with wider MTFs during the night. Sharpening this point, the question is whether the threshold imposed by practical instrumental limitations is lower or higher than the intersection between the two-phase function curves related to day and night. If the threshold is higher, the phase function related to the time of day, which

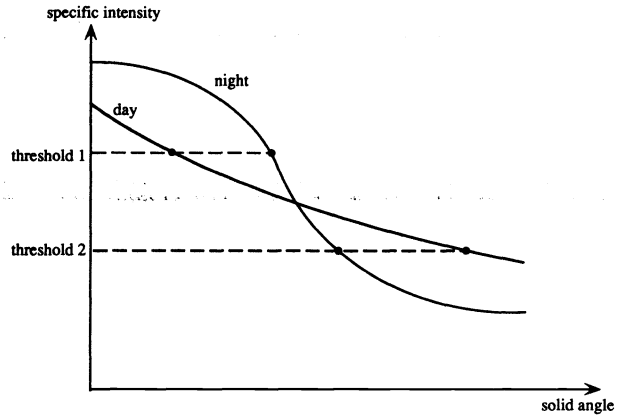

Fig. 14 Illustration of the system threshold imposed on different specific intensity functions.

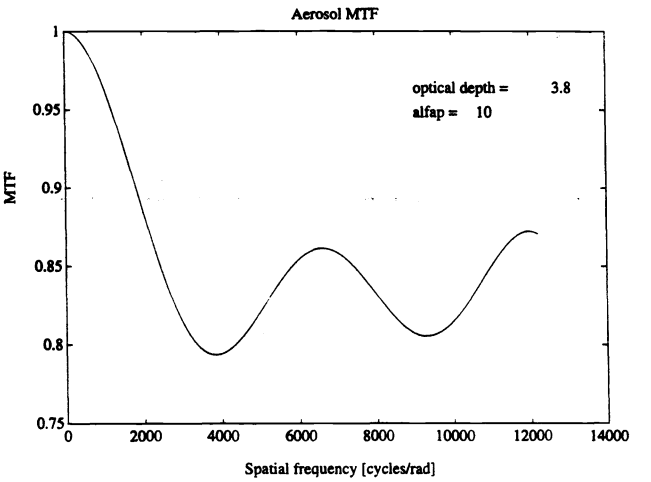

Fig. 15 Thermal IR aerosol MTF of 10-μm wavelength calculated for an imaging system with 16 cycles mrad^{-1} resolution.

is wider, is truncated earlier and the result is a wider MTF curve during the day. This analysis can be used to predict the variation in dynamic behavior of the limiting resolution imposed by the atmosphere on the basis of foreknowledge of meteorological parameters and their effect on aerosol size distribution.[11]

The effect of the spatial bandwidth is also examined. Because most new thermal imaging systems, particularly those using the FPA technology, are of significantly higher resolution performance (much above 1600 cycles/rad), calculations were made to examine this effect, as shown in Fig. 15. For wider spatial bandwidth systems, two main effects are important: (1) the direct effect of higher resolution achieved at the image plane and (2) the "improvement" in the recorded aerosol MTF at the image plane. These effects are mainly due to the larger amount of unscattered light recorded in the image, because the unscattered light goes up to an infinite angular spatial frequency while the scattered light is limited to Ω_c, as in Fig. 3. Therefore, the ratio between the unscattered light (corresponding to the unblurred image) and the scattered light (corresponding to the blurred image) is improved. We performed this analysis using a FPA imaging system with a spatial frequency bandwidth of 16 cycles mrad^{-1}. The severe limitation in this example was the background noise, which determines scene dynamic range, similar to that of the measurements shown here. In Fig. 15, alfap is the Gaussian scattering phase function parameter.[2,3] It appears that the aerosol MTF is much less dominant with regard to both a wider cutoff frequency and a higher asymptotic value at high spatial frequencies. Beyond the cutoff frequency, the aerosol MTF is not constant but has "ripples." Similar results for the aerosol MTF were obtained by Valley,[12] who used Monte-Carlo simulations and took into account the imaging system's limitations. In such high resolution systems, turbulence can be expected to be more significant,[13] although with less of a drop-off rate with spatial frequency than in the visible because of the longer IR wavelengths. While aerosol MTF is often more dominant than the turbulence MTF in the visible,[14] it can be expected to be even more so in the thermal IR, particularly because C_n^2 decreases with elevation above ground level, while for low elevations, aerosol size distribution is almost constant with elevation.

5 Image Restoration

Enhancement techniques for thermal images are summarized elsewhere.[15] Here, we concentrate on deblurring atmospheric effects.

Using the measured thermal IR atmospheric MTF, we applied several filtering techniques to thermal images recorded by the same imaging system to restore the blurred images. The most successful restorations were obtained by means of two different types of filters, and some results are presented here. Other spatial frequency filters, such as inverse and pseudoinverse filters, achieved less successful results. Figure 16 shows the results when the standard Weiner filter techniques were used based on both system and atmospheric MTFs. Figure 16(a) is the original picture as recorded by the Agema IR imaging system in the long-wave spectral range at a distance of about 1800 m. Figure 16(b) is the same image restored with the system MTF (Fig. 6) and with the atmospheric MTF measured simultaneously. Because the measured MTF did not vary significantly during the measurements, the use of an average atmospheric MTF is possible instead of measuring it when recording each new picture. This result is shown in Fig. 16(c). Note that both restored images are very much alike, indicating that the use of an average MTF is satisfactory and that it is very applicable when dealing with real-time image restoration. Measuring the MTF for each image is not necessary, thus limiting the processing time to the computation time.

Another technique that was used was the modified Backus-Gilbert filter,[16] which is a finite impulse response filter (FIR). Instead of simply optimizing the SNR as in the Weiner filter, this filter minimizes both the image blur and the noise energy. This technique is more adequate for the atmospheric problem because the distortion is modeled by a random filter and not a deterministic one, such as in the inverse and Weiner filters. The result of this filter is shown in Fig. 17, which is similar to that in Fig. 16 (FIR filter in the figure). Figure 18 shows the comparison of the Weiner and modified Backus-Gilbert filters, in which the simultaneous measured atmospheric MTF was used. Figure 19 shows a comparison of the results between the same two filters in which the average atmospheric MTF was used.

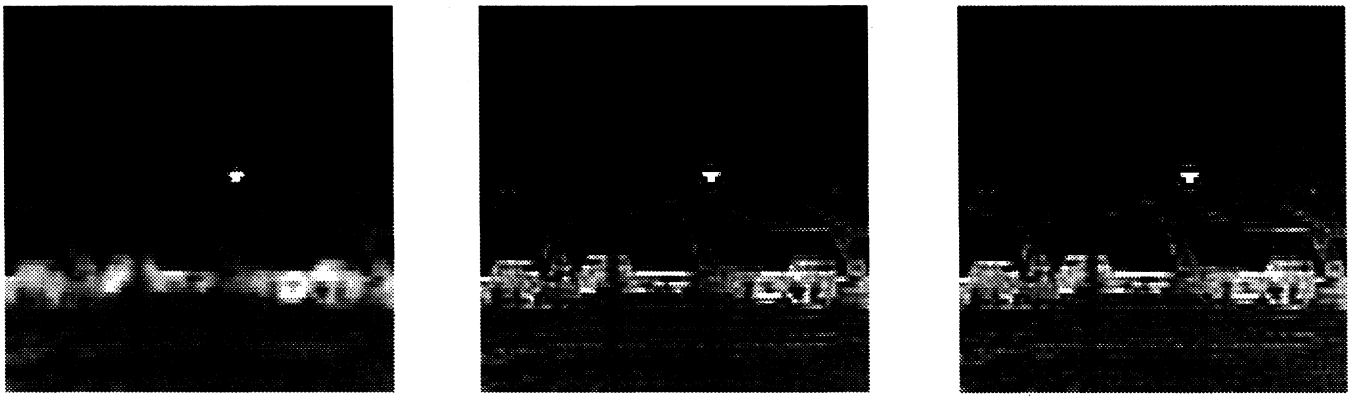

(a) (b) (c)

Fig. 16 Image restoration by means of the Weiner filter: (a) original picture, (b) restoration by means of a simultaneously measured MTF, and (c) restoration by means of an average atmospheric MTF.

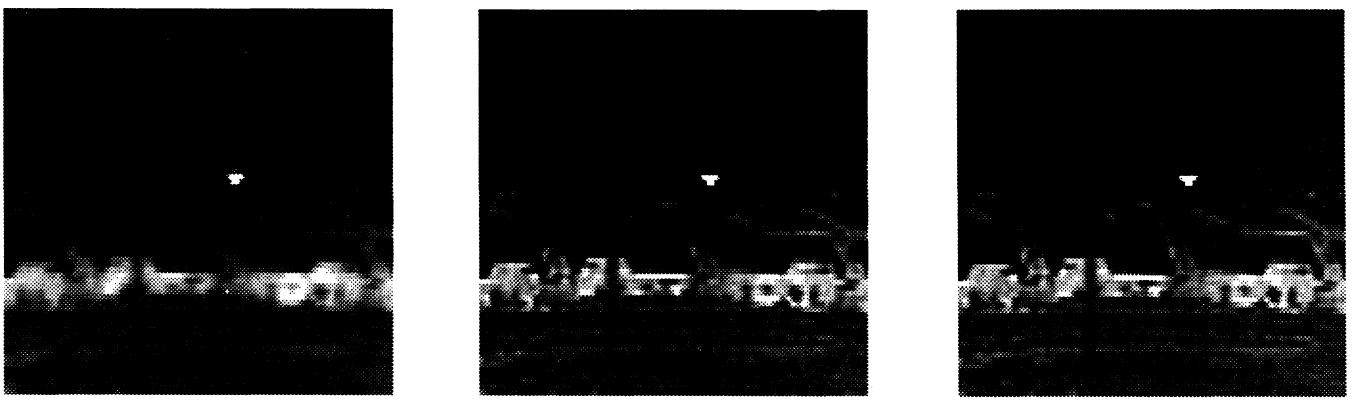

(a) (b) (c)

Fig. 17 Image restoration by means of the modified Backus-Gilbert spatial frequency filter: (a) original picture, (b) restoration by means of FIR filter, and (c) restoration by means of average atmospheric MTF.

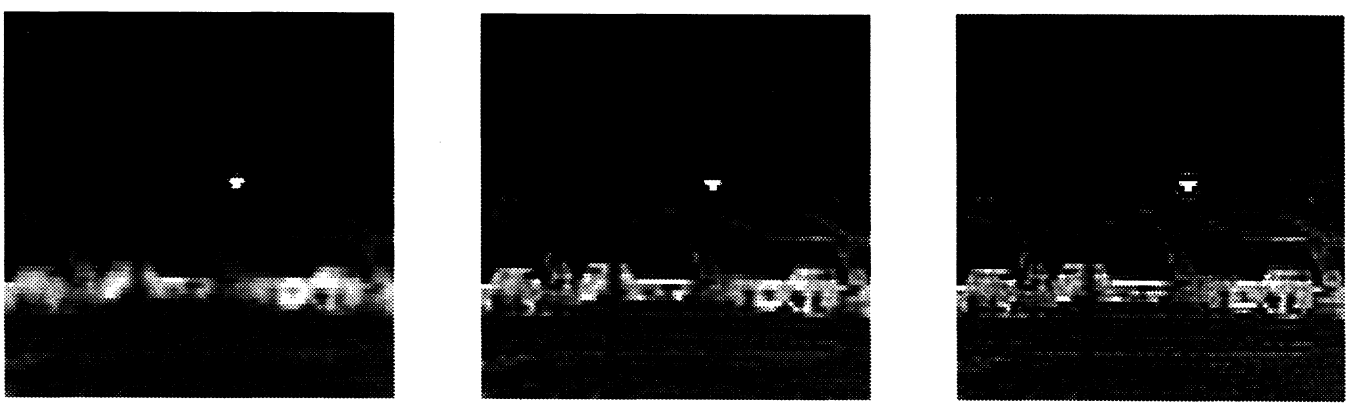

(a) (b) (c)

Fig. 18 Comparison of the Weiner and the modified Backus-Gilbert filter restorations using simultaneously measured atmospheric MTF: (a) original picture, (b) restoration with the FIR filter, and (c) restoration with the Weiner filter.

(a) (b) (c)

Fig. 19 Comparison between the Weiner and the modified Backus-Gilbert filter restorations using average atmospheric MTF: (a) original picture, (b) restoration with the FIR filter, and (c) restoration with the Weiner filter.

(a) (b) (c)

Fig. 20 Comparison between restorations: (a) original image, (b) restoration with the system MTF and (c) restoration with both system and atmospheric MTF.

In the restored images it is generally quite possible to see detail almost as small as a pixel dimension in the object plane (~62 cm), such as windows. This means that essentially all atmospheric blur is removed in the restoration process and the distant object scene is observed as if there were no atmosphere. This can only be possible by properly considering the atmospheric MTF and the significant role played by aerosol MTF. Such restoration does not depend on target shape. Rather, it is a fundamental image correction, which can be followed by other image processing techniques as required.

To examine the relation between the atmospheric and the imaging system's contribution to the overall blur imposed on the thermal image, we compared two types of image restoration: One was with a spatial frequency filter in which only the system's MTF (Fig. 6) was considered and that neglected the atmospheric MTF, and the other was with the measured MTF (including both system and atmospheric MTFs). Results of this comparison are shown in Fig. 20, which clearly shows that when the atmospherically derived blur is considered, the image restoration is significantly improved. This example demonstrates well that indeed a thermal atmospheric MTF exists and that the atmospheric effect should not be treated as a constant attenuation independent of spatial frequency. Target acquisition models should be revised.

In principle, a prediction of the aerosol size distribution[11] and the refractive index, together with instrumentation parameters, can be used to predict aerosol MTF. A model[9] for predicting turbulence MTF already exists, as does IMTURB. These models can be implemented in image restoration based on weather forecast.

6 Conclusions

Restoration of thermal images distorted by the atmosphere is presented based on spatial frequency filters and knowledge of the thermal IR atmospheric MTF. Such restoration is fundamental and yields an image quality limited essentially by hardware, as if there were no atmosphere. This is in contradiction to the conventional approach, which usually considers the atmospheric effect in the IR range as attenuation only, with no spatial frequency dependence considered. In addition, measured MTFs are presented for different meteorological

conditions and are obtained for different SNRs. Relating the atmospheric effect mainly to recorded aerosol MTF and taking into account the imaging system's limitations, we obtained results that are in very good agreement with theoretical predictions. This analysis can be used to predict the variation in dynamic behavior of the limiting resolution imposed by the atmosphere on the basis of foreknowledge of meteorological parameters and their effect on aerosol size distribution. In addition, we showed that the atmospheric MTF often does not vary much when the same imaging system is used, thus enabling the use of an average atmospheric MTF for the restoration techniques. Using the average atmospheric MTF to restore images, we achieved very good results. This is important when dealing with real-time image restoration, because the processing time can be limited to computational time only, with no simultaneous atmospheric measurements necessary. Knowledge of atmospheric MTF is essential to good cost-effective system design and is very useful in image restoration without any prior knowledge of the target to be viewed. In principle, atmospheric MTF can be predicted according to the weather forecast and implemented in image restoration accordingly.

Acknowledgment

This work was partially supported by the Ministry of Science and Technology, Jerusalem, Israel.

References

1. S. R. Rotman, E. S. Gordon, and M. L. Kowalcyzk, "Modeling human search and target acquisition performance: 3. Target detection in the presence of obscurants," *Opt. Eng.* **30**(6), 824–829 (June 1991).
2. D. Sadot and N. S. Kopeika, "Practical instrumentation-based theory and verification of aerosol MTF," *J. Opt. Soc. Am. A***10**(1), 172–179 (Jan. 1993).
3. D. Sadot and N. S. Kopeika, "Thermal imaging through the atmosphere: atmospheric MTF theory and verification," *Opt. Eng.* **33**(3), in press (1994).
4. J. W. Goodman, *Statistical Optics,* John Wiley & Sons, New York (1985).
5. A. Ishimaru *Wave Propagation and Scattering in Random Media,* Vol. 1, Academic Press, New York (1978).
6. R. F. Lutomirski, "Atmospheric degradation of electrooptical system performance," *Appl. Opt.* **17**(24), 3915–3921 (Dec. 1978).
7. A. Zardecki, S. A. W. Gerstl, and J. F. Embury, "Multiple scattering effects in spatial frequency filtering," *Appl. Opt.* **23**(22), 4124–4131 (Nov. 1984).
8. D. Sadot and N. S. Kopeika, "Effects of aerosol absorption on image quality through a particulate medium," submitted for publication.
9. D. Sadot and N. S. Kopeika, "Forecasting optical turbulence strength on the basis of macroscale meteorology and aerosols: models and validation," *Opt. Eng.* **31**(2), 202–212 (Feb. 1991).
10. R. F. Lutomirski and R. E. Warren, "Atmospheric distortion in a retroreflected laser signal," *Appl. Opt.* 14(4), 840–846 (1975).
11. I. Dror and N. S. Kopeika, "Prediction of particulate size distribution according to weather parameters," in *Atmospheric Propagation and Remote Sensing,* A. Kohnle and W. B. Miller, Eds., *Proc. SPIE* **1668,** 123–131 (1992).
12. M. T. Valley, "Numerical method for modeling nonspherical aerosol modulation transfer functions," in *Atmospheric Propagation and Remote Sensing,* A. Kohnle and W. B. Miller, Eds., *Proc. SPIE* **1668,** 73–85 (1992).
13. W. R. Watkins, S. B. Crow, and F. T. Kantrowitz, "Characterizing atmospheric effects on target contrast," *Opt. Eng.* **30**(10), 1563–1575 (1990).
14. I. Dror and N. S. Kopeika, "Aerosol and turbulence MTFs: Comparison measurements in the open atmosphere," *Opt. Lett.* **17,** 1532–1534 (Nov. 1992).
15. J. Silverman and V. E. Vickers, "Display and enhancement of infrared images," in *Electro-Optical Displays,* M. A. Karim, Ed., pp. 585–651, Marcel Dekker, Inc., New York (1992).
16. R. K. Ward and B. E. A. Saleh, "Deblurring random blur," *IEEE Trans. Acoust. Speech Sig. Process.* **ASSP-35**(10), 1494–1497 (Oct. 1987).

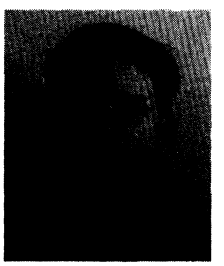

Dan Sadot received his BSc and MSc degrees in electrical and computer engineering from Ben Gurion University of the Negev, Beer-Sheva, Israel, in 1988 and 1991, respectively. He is now a PhD student in the Electrical and Computer Engineering Department of Ben Gurion University and is also part of the Electro-Optic Program Research Group. His current research is on atmospheric optics, turbulence effects, aerosol light scattering and application to imaging systems, restoration of images distorted by the atmosphere, optical atmospheric coherence diameter, and effects of atmospheric blur in target acquisition probabilities.

A. Dvir: Biography and photograph not available.

I. Bergel: Biography and photograph not available.

Norman S. Kopeika received the BS, MS, and PhD degrees in electrical engineering from the University of Pennsylvania, Philadelphia, in 1966, 1968, and 1972, respectively. His PhD dissertation, supported by a NASA Fellowship, dealt with detection of millimeter waves by glow discharge plasmas and the utilization of such devices for detection and recording of millimeter wave holograms. In 1973 he joined the Department of Electrical and Computer Engineering, Ben-Gurion University of the Negev, Beer-Sheva, Israel, where he is a professor. In 1978 and 1979 he was a visiting associate professor in the department of Electrical Engineering, University of Delaware, Newark. He has published more than 80 journal papers. He has been particularly active in research of time response and impedance of properties of plasmas and has also authored a general unified theory to explain EM wave-plasma interactions all across the electromagnetic spectrum. Recently, he has contributed toward characterizing the open atmosphere in terms of an MTF with which to describe effects of weather on image propagation. Kopeika is a senior member of IEEE and a member of SPIE, OSA, and the Laser and Electrooptics Society of Israel.